I&EC research
Industrial & Engineering Chemistry Research

Article

pubs.acs.org/IECR

Interactive Effect for Simultaneous Removal of SO_2, NO, and CO_2 in Flue Gas on Ion Exchanged Zeolites

Hua Deng,[†] Honghong Yi,*[,‡,§] Xiaolong Tang,[‡,§] Haiyan Liu,[§] and Xuan Zhou[§]

[†]Research Center for Eco-Environmental Sciences, Chinese Academy of Sciences, Beijing, 100085, China

[‡]College of Civil and Environmental Engineering, University of Science and Technology Beijing, Beijing 100083, China

[§]Faculty of Environmental Science and Engineering, Kunming University of Science and Technology, Kunming 650500, China

Supporting Information

ABSTRACT: A purification system for simultaneous removal of SO_2, NO, and CO_2 in flue gas was considered in this study. For improving the purification performance of candidate adsorbent NaX zeolite, ion exchange experiments were conducted with cation K^+, Ca^{2+}, Mn^{2+}, and Co^{2+}, respectively. The texture properties of series zeolites were examined by N_2 porosimetry, X-ray diffraction (XRD), and X-ray photoelectron spectroscopy (XPS) analyses. Among the sorbents investigated, K−NaX zeolite exhibited the best result to remove SO_2, NO, and CO_2 all together. XPS results revealed that SO_2 has been oxidized to form SO_4^{2-} on the solid surface; however, species N and C have not been observed. In order to understand the coadsorption effects, pure component, binary, ternary components, and mimic flue gas breakthrough experiments were designed and carried out. It suggested that SO_2 and NO was bonded on the adsorbent surface with degradation of NO. A little competitive effect of CO_2 on SO_2 and NO adsorption system were found. Finally, monitoring of coadsorption venting gas, thermodynamic equilibrium species simulation, TPD experiment, and quantum chemical calculation technology were used to examine the interactive effect.

1. INTRODUCTION

Flue-gas emissions in the atmosphere deriving from combustion processes pose today serious environmental concerns. Due to the progressive industrialization of the planet, over 85% of the energy demand is currently supplied by fossil fuels.[1] It was reported that more than 98% of SO_2,[2] over 90% of NO_x,[3] and 71% of CO_2[4] emission are mainly generated from the combustion of fossil fuels. SO_2 and NO_x are toxin gases and directly responsible for the acid rain, photochemical smog, and other atmosphere environmental problems. Moreover, CO_2 and NO_x are recognized as two main greenhouse gases, which pose the threat that the global temperature will be in the range of 1.4−5.8 °C and sea level will rise of 9−88 cm by the end of this century.[5]

To avoid all these catastrophic environmental problems, many technologies such as flue gas desulfurization (FGD), selective catalytic reduction (SCR), and carbon capture and storage (CCS) have therefore been developed.[2−6] However, they are often multistep, complex, and costly processes. Thus attempts have been made to find a suitable method for removal SO_2, NO, and CO_2 in flue gas simultaneously.[7] In our former research,[8] a new adsorption system was constructed. It was demonstrated that adsorption technology is a very attractive way to treat multicomponent gaseous mixtures.

There are several adsorbents that show very promising future in flue-gas purification field. Zeolites, which are commonly used for gas separation and catalysis,[8] were considered in this study. For improving the performance of the adsorbent, the ion exchange chemical modification method was adopted. Carbon capture by adsorption methods through ion exchange zeolite have been extensive studied,[9,10] and the optimum ion species are alkalis especially K^+.[11] Other literatures[12,13] also reported that ion exchanged zeolite have high NO adsorption capacity such as ion Co and Mn. In this study, ion K, Ca, Mn, and Co were selected to investigate the nature of coadsorption. Even through there are some literature works[14,15] referring to simultaneous removal of SO_2 and NO in flue gas, there are no papers concerning simultaneous removal of SO_2, NO, and CO_2 by adsorption methods. How multicomponents in flue gas interact with each other or a specific adsorbent would be an interesting and important issue.

Thus, the objective of this study is fourfold. (1) A series of ion exchanged NaX zeolites were prepared, and the characterizations including X-ray diffraction (XRD), Brunauer−Emmett−Teller (BET), and X-ray photoelectron spectroscopy (XPS) were summarized. (2) The purification experiment of SO_2, NO, and CO_2 were conducted, and the best performed adsorbent was picked out. (3) Multicomponent coadsorption effects were found by binary and ternary component and mimic flue gas breakthrough experiments. (4) The co-adsorption mechanism was elicited through thermo-equilibrium species simulation, temperature-programmed desorption (TPD) results and quantum chemical calculations.

2. MATERIALS AND METHODS

2.1. Material Preparation. Zeolite samples (NaX) used in this work were pellets (2.5−5 mm) from the catalyst plant of Nankai University, Tianjin, China. Ionic exchange was carried out by stirring 20 g of parent zeolite in 200 mL of aqueous solution containing 0.1 mol L^{-1} of the metal chloride or nitrate

Received: December 3, 2012
Revised: April 15, 2013
Accepted: April 16, 2013
Published: April 16, 2013

dx.doi.org/10.1021/ie303319f | Ind. Eng. Chem. Res. 2013, 52, 6778−6784

salt (KCl, $CaCl_2$, $Mn(NO_3)_2$, $Co(NO_3)_2$), respectively. The mixture was agitated on a rotary shaker for 2 h at 333 K in a water bath. The procedure was repeated three times, and each exchange was conducted with fresh solution. After filtering with deionized water, ion exchanged samples were dried overnight in air at 393 K. The final dried exchanged samples were activated in a tube furnace in the protection of N_2 with the flow of 300 mL min^{-1}. The samples were heated in the furnace up to 673 K at 1 K min^{-1} and maintained at the maximum temperature for 12 h to remove water. A sample M−NaX indicates a zeolite which derives from the NaX sample and is exchanged with M ion.

2.2. Experiments. *2.2.1. Adsorbent Characterization.* The X-ray powder diffraction patterns of the various adsorbents were collected on a D/Max2200 X-ray powder diffractometer (Ricoh, Japan). The patterns were run with Ni-filtered Cu radiation (λ = 1.5406 Å) at 36 kV and 30 mA with a scanning speed of 5°/min. Nitrogen adsorption−desorption isotherms were measured using Micromeritics Instrument TriStar II 3020 V1.03 at 77 K. The specific surface area of the samples was calculated by the Brunauer−Emmett−Teller (BET) method. The volume of pores was determined by the single-point method.[16,17] In order to obtain the ion exchange degree, elemental analysis of the M−NaX was conducted by Vririan SpectrAA220 FS. The ion exchange degree was defined as the difference between parent zeolite and exchange sample in the means of Na amont. XPS analyses were performed by means of a X-ray used Al Kα radiation with energy of Al rake and power of 200 W. The continuum spectrum was fitted according to the Gaussian−Lorentzian files.

2.2.2. Breakthrough Experiments. A schematic diagram of the laboratory system used for measuring breakthrough curve was set up and shown in our former work.[8] The adsorber consists of a quarz glass tube of 18 mm i.d. and 200 mm length, and it was placed in a tubular heater with accuracy ±1 °C in order to control the temperature test. SO_2, NO, and CO_2 were supplied by pressurized cylinder. The former ion exchanged zeolites were crushed and sieved into 0.35 mm; all hinder effects have been eliminated. Concentration for SO_2, NO, CO_2, and the N_2 cylinder were 1%, 1%, 99.9%, and 99.99% (vol %), respectively. Delivery of the feed gas was controlled by mass flowmeters. After mixing in a mixing tank, simulated gas was fed into the inlet of the quartz glass reactor. Prior to all measurements, an initial degassing of the sample was performed at 120 °C under the flow of nitrogen overnight. Then mixed gas was passed through the fixed bed column at constant temperature. The inlet and outlet concentration were analyzed by a Kane KM9106 flue gas analyzer with an additional infrared module, which has resolution for SO_2, NO, and CO_2 of 1 ppm, 1 ppm, and 0.1%, respectively. Dynamic experimental conditions employed in these measurements were detailed in S1 (Supporting Information). The total flow was kept constant, and the SO_2, NO, and CO_2 was controlled precisely according to S1 with balance gas N_2 during binary and ternay experiments. For comparing the adsorption efficiency, the dynamic adsorption capacity of the column was calculated using eq 1:

$$q = \frac{FC_0t_q}{22.4W} \tag{1}$$

Where q is the adsorption amout (mmol g^{-1}), F is the total molar flow (ml min^{-1}), C_0 is the concentration of the adsorbate in the feed steam (ppm for SO_2, NO; vol % for CO_2), W is the mass of adsorbent loaded in the column (g), and t_q is the stoichiometric time (min), which is estimated from the breakthrough profile according to eq 2:[18]

$$t_q = \int_0^\infty \left(1 - \frac{C_A}{C_0}\right) dt \tag{2}$$

3. RESULTS AND DISCUSSION

3.1. Characterizations of Ion Exchanged Zeolites. Characterizations of the representative adsorbents namely bare zeolite NaX and zeolite NaX exchanged with ion solution of several kinds of cation were studied. The effect of ion exchange loading on the structural properties of zeolite matrix was investigated by obtaining XRD patterns. From the X-ray diffractogram of cation incorporated zeolite in Figure 1, it can

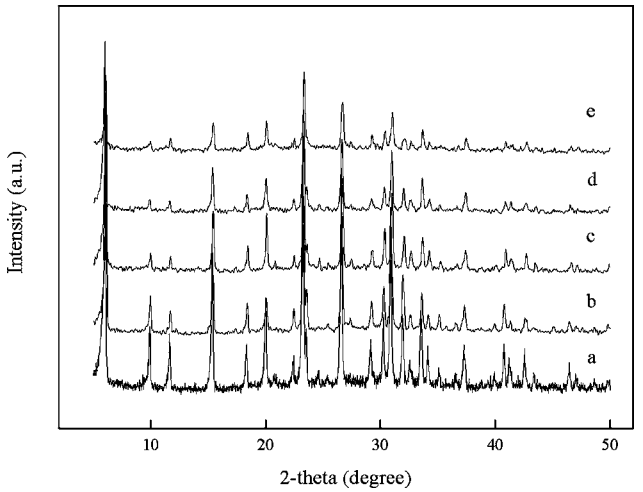

Figure 1. XRD patterns of NaX, K−NaX, Ca−NaX, Mn−NaX, and Co−NaX zeolite: (a) NaX, (b) K−NaX, (c) Ca−NaX, (d) Mn−NaX, (e) Co−NaX.

be observed that the structural integrity of parent zeolite is maintained even after several times of ion exchange. All samples exhibit characteristic peaks of zeolite NaX with no other impurity phase.[16] Upon ion-exchange by various cations, the intensities of the characteristic peaks were significantly reduced. This might be ascribed to the partial blocking of pores and decreased crystalline of the structure by incorporation of cations.[19,20]

In order to confirm the extent of ion exchange, which is very important for the analysis of cation effect, element analysis was conducted by Na atom absorption spectrum as described in section 2.2.1. The results were summarized in S2 (Supporting Information). As shown, a bivalent cation (Ca^{2+}, Mn^{2+}, Co^{2+}) enables a higher degree of ion-exchange than a univalent cation (K^+). Since their +2 charge, only the half as much as in alkali metal ions are needed for complete ion exchange despite the size problem, which enables a high degree of exchange. Due to the relatively large ion size, it is more difficult for Mn^{2+} and Co^{2+} to achieve higher exchange degree than cation Ca^{2+}. The sum of diffusion problems and ion-exchange sites located within the micropores may function in the ion exchange process. The same trend was found between our results and other literature works where the large ions and univalent ions possess relatively low exchange degree.[9,11,21] Textural properties of the samples were also shown in S2. All ion-exchange

dx.doi.org/10.1021/ie303319f | Ind. Eng. Chem. Res. 2013, 52, 6778−6784

zeolites exhibited smaller surface area and pore volume compared to parent zeolite. The decrease of surface area and pore volume may attribute to the exchanged ions being partly block the pore mouth, then accessible space are limited. K−NaX and Ca−NaX zeolites were still dominated by micropore; however, Mn−NaX and Co−NaX were no longer microporous.

3.2. Effect of Ion Exchange in Purification of SO_2, NO, and CO_2. In order to understand the significance of ion exchange on the performance of coadsorbing SO_2, NO, and CO_2 simultaneously, coadsorption results were measured by using breakthrough method. The results and experimental conditions were plotted in Figure 2. In the field of purification flue gas by adsorption method, pollutant removal efficiency can partly equal to adsorption amounts. For comparing the differences in removal efficiency quantitatively, breakthrough adsorption capacities were calculated and summarized in Table 1 as described in section 2.2.2. It is noteworthy that calculation amount of the breakthrough experiments is defined at a break point of 95% C/C_0 for all runs. As the breakthrough curves show, SO_2 presents the best purification effect among the three pollutants. NO only shows removal efficiency of about 20% from the starting point to 200 min later. CO_2 is under an inferior position in the coadsorption system because it breaks through the adsorbent bed quickly, and no net removal efficiency is clearly found. However, it exhibits the highest adsorption amount among the pollutants due to its relative higher partial pressure. The higher CO_2 concentration with respect to the inlet one can be ascribed to the displacement of CO_2 molecules by SO_2 and NO (roll-up effect), and it was also observed in a former study of our research group.

Among all the zeolites studied, the adsorption amounts of K−NaX are improved except for CO_2 according to Table 1. However, the rest of the ion-exchange zeolites do not present superior performance in simultaneous purification of SO_2, NO, and CO_2 than the parent zeolite. The apparent reason would be that the surface area and pore volume have been reduced to a great extent, which derives from the ion-exchange process. In order to figure out if the paradox lays in K−NaX, samples of fresh NaX, K−NaX, and K−NaX zeolite that has been used for coadsorption were examined by X-ray photoelectron spectra. The binding energy data are listed in Table 2.

It can be observed from the table that all binding energy of Al, Si, and Na element in NaX are consistent with the X type zeolite. Through the metal cation exchange, K element is apparently found on the surface of NaX zeolite. In general, a reduced ionicity shifts the binding energies to lower values[22] and so also by analogy to some cations exchanged on molecular sieves.[23] We tentatively assigned element K to metal oxide-like structures. They must form some chemical state of K_2O_2 or K_2O_3 because the O1s binding energy of K_2O is 528.5 ev.[24,25] Another clue also testifies our observation is that O1s binding energies of NaX and tested K−NaX are very close and different from that of K−NaX. K−NaX presents the lowest binding energy of O1s, and it indicates that bonded K may present relative less O surrounding envriomeent. The main difference between fresh and tested K−NaX is that tested zeolite has been undergone an atmosphere of 5% O_2 surrounded. Through an oxidation reaction, the fresh K−NaX has bonded with O_2 on the surface then the binding energy increased. In a word, K cation exchange creates a reduced chemical environment for the the NaX zeolite, which is the main cause of its superior performance in purification of SO_2 and NO. After coadsorption of SO_2, NO, and CO_2, elemental S was found on the surface of the K−NaX zeolite but for elemental N and C by XPS experiment. According to Table 2, we can conclude that SO_2 has followed an oxidation to SO_4^{2-} since the binding energy is 169.73 ev, which is the feature binding energy of SO_4^{2-}.[8] Unlike most known routine of oxidation of NO with SO_2 in flue gas[26] to form NO_3^-, elemental N was not monitored on

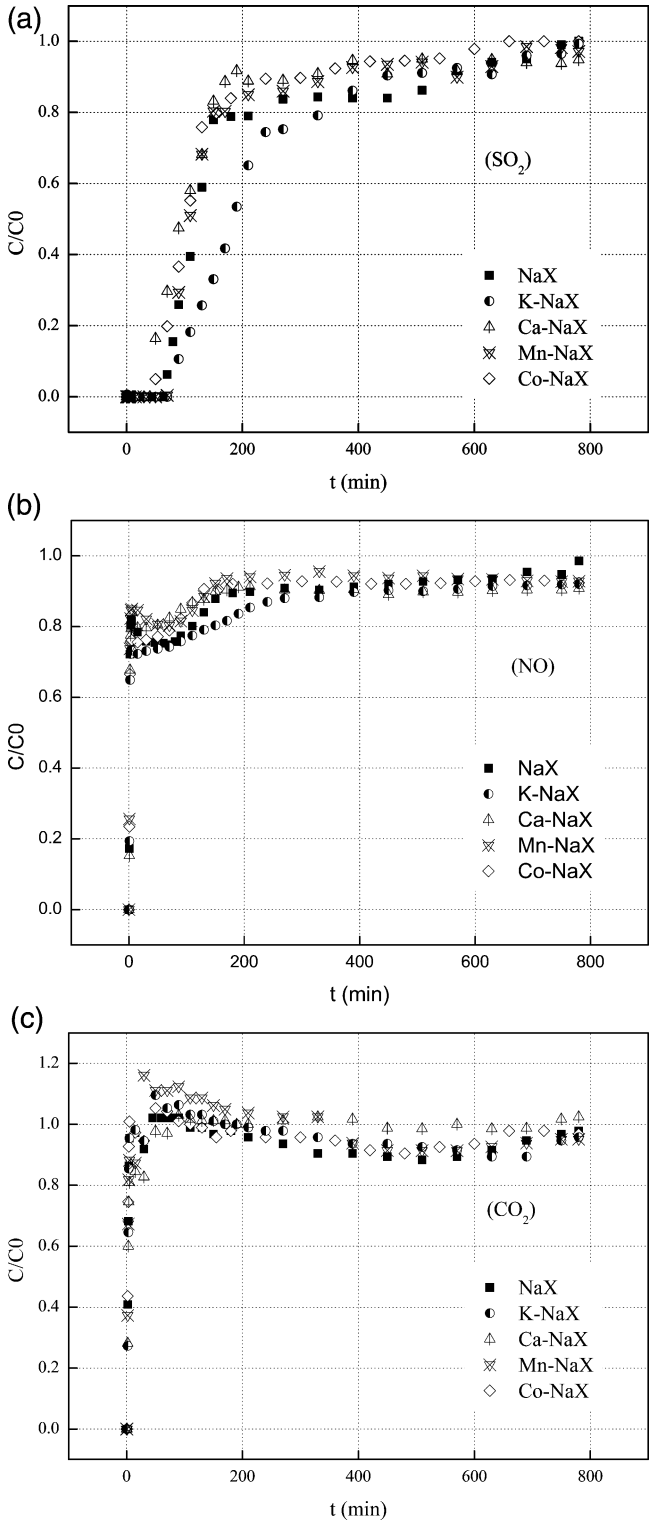

Figure 2. Breakthrough curves for SO_2, NO, and CO_2 on NaX, K−Nax, Ca−NaX, Mn−NaX, and Co−NaX zeolite: (a) SO_2, (b) NO, (c) CO_2. Experimental conditions: SO_2 2000 ppm, NO 1000 ppm, CO_2 10%, O_2 5%, N_2 balance.

dx.doi.org/10.1021/ie303319f | Ind. Eng. Chem. Res. 2013, 52, 6778−6784

Table 1. Dynamic Adsorption Amount for Ion Exchange Zeolites

($mmol\ g^{-1}$)	SO_2	NO	CO_2
NaX	1.29	0.27	17.41
K−NaX	1.59	0.35	12.17
Ca−NaX	0.98	0.29	2.38
Mn−NaX	1.12	0.21	4.85
Co−NaX	0.95	0.25	11.6

Table 2. XPS of Zeolites NaX, K−NaX, and K−NaX after Coadsorption Experiments

nature form (ev)	NaX	K−NaX	K−NaX (tested)
Al (2p) (72.95, 72.55)	74.76	74.59	75.01
Si (2p) (99.82, 99.42)	(103.17, 101.40)	(102.97, 101.32)	(102.97, 100.94)
Na (1s) (1070.8)	1072.26	1071.87	1071.76
K (2p) (297.3, 294.6)		(296.43, 293.59)	(296.44, 293.58)
O (1s) (543.1)	(533.00, 531.73)	(532.91, 531.58)	(532.96, 531.72)
S (2p) (163.6, 162.5)			169.73

the surface of sample, thus molecule NO probably went through a different mechanism and may have been reduced to N_2 then in the effluent.

3.3. Coadsorption Effect of Multiple Components. In order to understand the multicomponent interaction effect, coadsorption experiments were designed and analyzed. The results were presented in Figure 3. The dynamic adsorption amount of the interaction effect was calculated and listed in Table 3 to aid understanding of the detailed mechanism.

As Figure 3 and Table 3 show, K−NaX zeolite has the highest purification efficiency of SO_2 among the three pure pollutants. NO and CO_2 show a fast breakthrough, and little adsorption amounts were observed in the pure component adsorption experiments. When the interaction effect of SO_2 and NO was considered, a very interesting phenomenon appeared. After the initial breakthrough, the NO concentration descends to a minimum and then gradually ascends with the breakthrough starting point of SO_2. This result definitely proves that SO_2 and NO promote the adsorption of each other also proved in Table 3. Given that there are element S sticks on the samples after adsorption, however, no element N was observed through XPS experiment. Molecule NO should react with SO_2 on the zeolite in a reduction way to form certain reductive species. When the CO_2 component is added to the SO_2 and NO

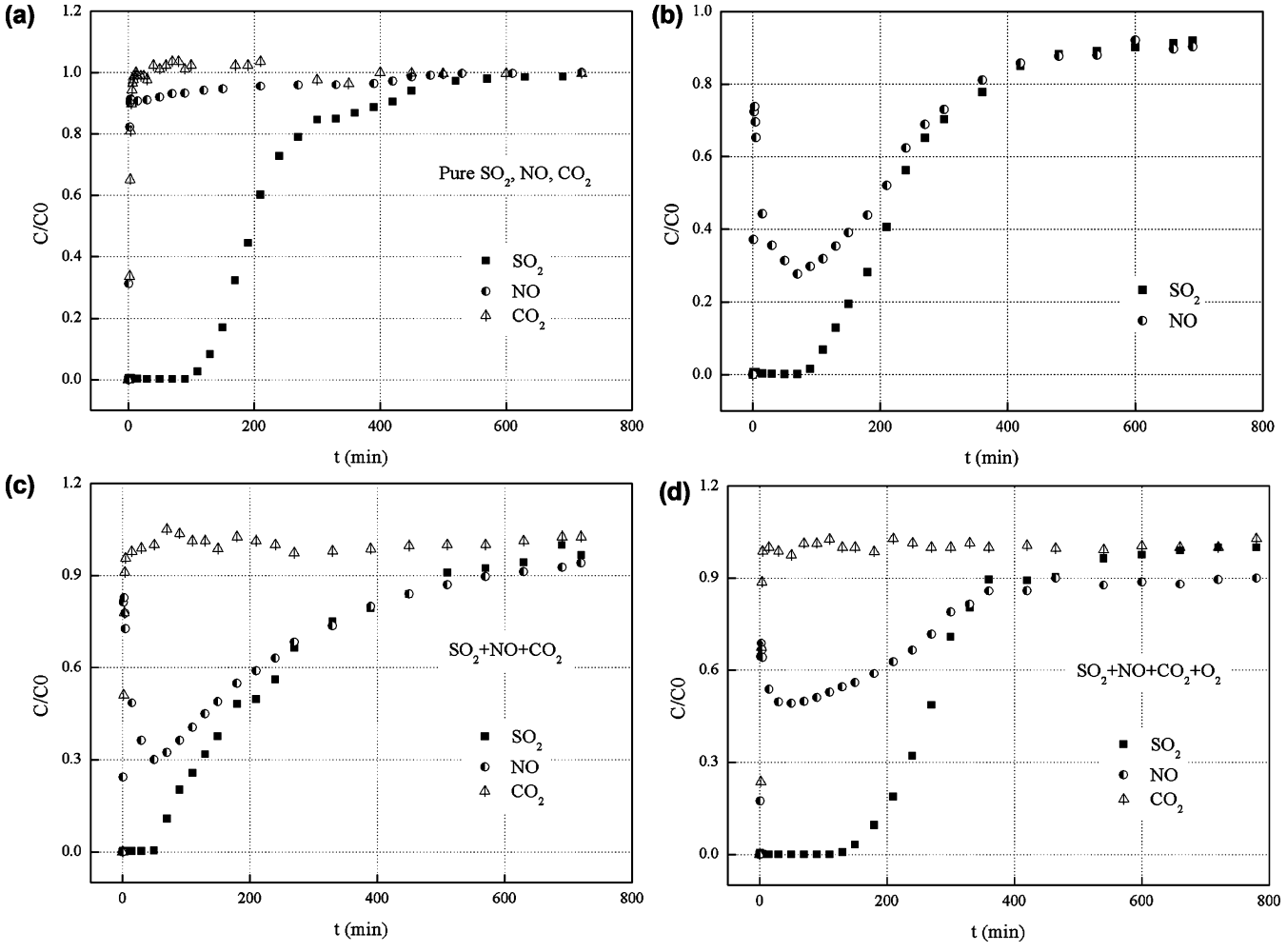

Figure 3. Coadsorption breakthrough curves for SO_2, NO, and CO_2 on K−NaX zeolite: (a) pure SO_2, NO, CO_2 (SO_2 2000 ppm/NO 1000 ppm/CO_2 10%, N_2 balance), (b) SO_2 + NO, (SO_2 2000 ppm, NO 1000 ppm, N_2 balance), (c) SO_2 + NO + CO_2, (SO_2 2000 ppm, NO 1000 ppm, CO_2 10%, N_2 balance), (d) SO_2 + NO + CO_2 + O_2 (SO_2 2000 ppm, NO 1000 ppm, CO_2 10%, O_2 5%, N_2 balance).

dx.doi.org/10.1021/ie303319f | Ind. Eng. Chem. Res. 2013, 52, 6778−6784

Table 3. Interaction Effect of SO_2, NO, and CO_2 on Dynamic Adsorption Amount

coadsorption interaction experiment	single component in mixture	dynamic adsorption amount (mmol g^{-1})
pure component (SO_2, NO, CO_2)	SO_2	1.54
	NO	0.083
	CO_2	0.51
two component (SO_2+NO)	SO_2	1.87
	NO	0.72
triple component (SO_2 + NO + CO_2)	SO_2	1.66
	NO	0.69
	CO_2	0.28
mimic flue gas (SO_2 + NO + CO_2 + O_2)	SO_2	1.77
	NO	0.61
	CO_2	0.13

adsorption system, the trend for SO_2 and NO has never been changed except for the little reduction of relative adsorption amounts. It suggests that CO_2 have limited effect on the adsorption of SO_2 and NO. For the mimic flue gas, O_2 was taken in account as a very important factor due to its good oxidation capacity. As shown in Figure 3, the trend of NO has been changed and did not proceed in the adsorption bed with the accordance with SO_2. It seems that O_2 in the flue gas substitutes part of the function of NO. It in another way demonstrates that NO as an oxidant reacts with SO_2 on the surface of K−NaX zeolite. In other words, NO was supposed to be reduced to N_2 or N_2O with oxidation of SO_2 to SO_3.

3.4. Mechanism of Coadsorption. For proving the observations and supposiotions above, thermodynamic calculation was adopted to simulate our adsorption system. According to results of the equilibrium species searching by sofeware Factsage 6. SO_2 was oxidized to form SO_4^{2-}, which is consistent with our experimental findings. However, N_2 was the equilibrium states for NO not N_2O. The other experimental evidence can also support the simulation. The vending gases in NO purification phase during the coadsorption experiment were also monitored by Thermo fisher infrared flue gas analyzer (Thermo Antaris IGS Analyzer), which can test N_2O with resolution of 1 ppb. The result reveals that only 54 ppm N_2O were found. It can be concluded that the most purified NO in flue gas was converted to N_2.

A simple temperature program desorption experiment apparatus was also constructed. After the coadsorption experiment, the sample K−NaX zeolite was immediately transferred to the TPD tank with helium mass flow of 300 mL/min. In the first 5 min, the temperature was kept at the ambient. Then, the heater started to heat up at a rate of 3 K/min. The vent was monitored with our Flue Gas Analyzer online (Kane KM9605). The result was plotted in Figure 4. There are two interesting aspects of the results needed to be noticed. First, through the mass balance analysis, a few NO was observed through TPD experiment. Thus, the massive purified NO must be degenerated. This finding also supports the conversion phenomenon of NO in flue gas. Second, NO desorbed at a relatively low temperature, and started with the low temperature desorption peak of SO_2. This result also proves that there is no NO^{3-} or NO^{2-} species on zeolite surface.[27,28] Thus, purified NO must be conversed in a reductive way. The TPD experiment testifies our observation about the conversion of NO in flue gas.

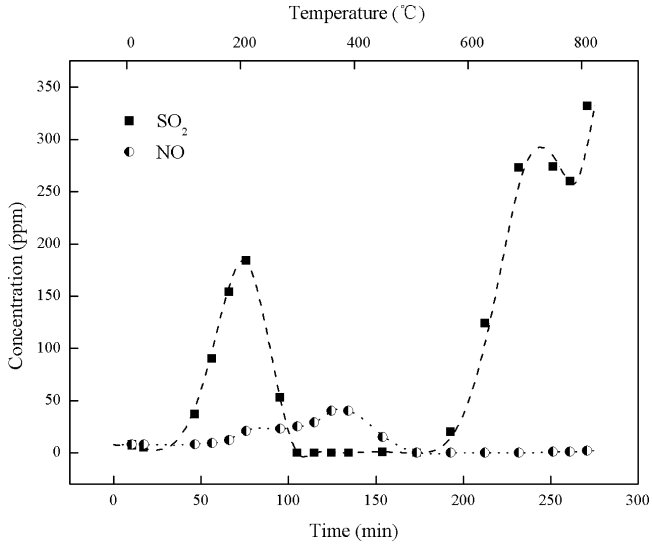

Figure 4. Temperature-programmed desorption profiles of K−NaX zeolie.

It was reported that SO_2 and NO were physi-adsorbed on zeolites.[29−32] Our former work also exhibited the same feature.[7,8] Thus we can make an assumption that the K−NaX zeolite only worked as a field, which concentrated the adsorbates and did not change their chemical properties on the surface of zeolites. Considering the coadsorption effect analyzed above, a mechanism can be drawn as follows:

Overall reaction

$$2SO_{2(ad)} + 2NO_{(ad)} \rightarrow 2SO_{3(ad)} + N_{2(ad)}$$

In order to understand the detailed reaction at the molecular level, quantum chemical calculation was carried out using Gaussian 03 package.[33] As a reasonable compromise between accuracy and computational time, the geometries of reactants, transition states, and reaction path were fully optimized by employing the b3lyp method with a 311-g (d, p) basis set. The transition state of the first elementary reaction was found. The intrinsic reaction coordinate (IRC) routines were presented in Figure 5. This proved that the mechanism of the coadsorption effect was reasonable and gave us a vivid insight into how SO_2 and NO functioned in the system. As shown in Figure 5, the details about the reaction can be proved as follows:

Elementary reaction 1

$$SO_{2(ad)} + NO_{(ad)} \rightarrow SO_3N_{(ad)}$$

According to the frontier theory, intermediate SO_3N can not react with NO because the high frontier orbital energy gap between them, however, two intermediates SO_3N can follow the path according to the frontier theory:

Elementary reaction 2

$$SO_3N_{(ad)} + SO_3N_{(ad)} \rightarrow 2SO_3 + N_2O_{(ad)} + SO_{2(ad)}$$

Elementary reaction 3

$$N_2O_{(ad)} + SO_{2(ad)} \rightarrow SO_{3(ad)} + N_{2(ad)}$$

Adsorbed $SO_{3(ad)}$ would react with the element O in zeolite and turn to SO_4^{2-}, while most NO convert to harmless N_2. A small amount of N_2O still can be found in the vending gas. It can be concluded that the mechanism is consistent with the

dx.doi.org/10.1021/ie303319f | Ind. Eng. Chem. Res. 2013, 52, 6778−6784

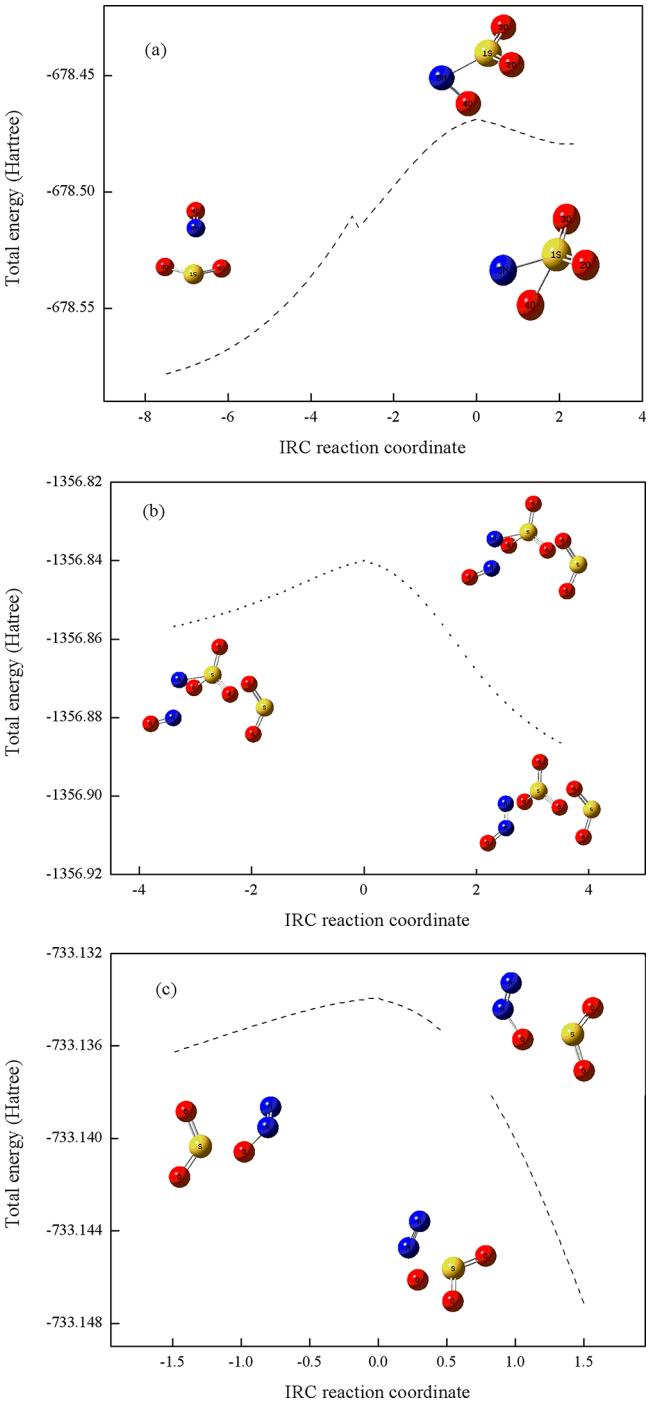

Figure 5. IRC curves and intermediate structures for reaction of SO_2 and NO: (a) $SO_{2(ad)} + NO_{(ad)} \rightarrow SO_3N_{(ad)}$, (b) $SO_3N_{(ad)} + SO_3N_{(ad)} \rightarrow 2SO_3 + N_2O_{(ad)} + SO_{2(ad)}$, (c) $N_2O_{(ad)} + SO_{2(ad)} \rightarrow SO_{3(ad)} + N_{2(ad)}$.

experiment findings that $SO_{2(ad)}$ and $NO_{(ad)}$ bonded on the zeolite surface and the chemical bond between NO were cleaved. For deep understanding, further investigation will be necessary in field of chemical role which the zeolite played in the adsorption system.

■ ASSOCIATED CONTENT

Supporting Information

Table S1: experimetal conditions for breakthrough curves. Table S2: ion exchanged degrees and textural parameters of zeolites. This material is available free of charge via the Internet at http://pubs.acs.org.

■ AUTHOR INFORMATION

Corresponding Author

*Tel.: +86 10 62332747. E-mail: yhhtxl@163.com.

Notes

The authors declare no competing financial interest.

■ ACKNOWLEDGMENTS

The work was supported by the National Natural Science Foundation of China (21077047) and Program for New Century Excellent Talents in University (NCET-12-0776).

■ REFERENCES

(1) Yang, H. Q.; Xu, Z. H.; Fan, M. H. Progress in carbon dioxide separation and capture: A review. *J. Environ. Sci.* **2008**, *20*, 14.
(2) Probstein, R. F.; Hicks, R. E. *Synthetic Fuel*; Dover Publication: New York, 2006.
(3) Zhu, J. L.; Wang, Y. H.; Zhang, J. C. Experimental investigation of adsorption of NO and SO_2 on modified activated carbon sorbent from flue gases. *Energy Covers. Manage.* **2005**, *46*, 2173.
(4) Xu, X. C.; Chen, C. H.; Qi, H. Y. Development of coal combustion pollution control for SO_2 and NO_x in China. *Fuel Process. Technol.* **2000**, *62*, 153.
(5) Houghton, J. T.; Ding, Y.; Griggs, D. J.; Noguer. *IPCC Climate Change 2001: The Scientific Basis, Intergovernmental Panel on Climate Change*; Cambridge University Press: Cambridge, U. K., 2001.
(6) Liu, Y.; Bisson, T. M.; H. Yang, Q. Z.; et al. Recent developments in noval sorbents for flue gas clean up. *Fuel Process. Technol.* **2010**, *91*, 1175.
(7) Deng, H.; Yi, H. H. Adsorption equilibrium for sulfur dioxide, nitric oxide, carbon dioxide, nitrogen on 13X and 5A zeolites. *Chem. Eng. J.* **2012**, *188*, 77.
(8) Yi, H. H.; Deng, H.; Tang, X. L. Adsorption equilibrium and kinetcs for SO_2, NO, CO_2 on zeolites FAU and LTA. *J. Hazard. Mater.* **2012**, *203–204*, 111.
(9) Zhang, J.; Singh, R.; Webley, P. A. Alkali and alkaline-earth cation exchanged chabazite zeolites for adsorption based CO_2 capture. *Microporous Mesoporous Mater.* **2008**, *111*, 478.
(10) Walton, K. S.; Abney, M. B.; LeVan, M. D. CO_2 adsorption in Y and X zeolites modified by alkali metal cation exchange. *Microporous Mesoporous Mater.* **2006**, *91*, 78.
(11) Yang, S.-T.; Kim, J.; Ahn, W.-S. CO_2 adsorption over ion-exchanged zeolite beta with alkali and alkaline earth metal ions. *Microporous Mesoporous Mater.* **2010**, *135*, 90.
(12) Zhang, W.-X.; Jia, M.-J. Adsorption Properties of Nitrogen Monooxide on Metal Ion-exchanged Zeolites. *Chem. J. Chin. Univ.* **1997**, *18*, 1999.
(13) Xue, Q.; Zhang, Y.; Song, W. Low concentration NO adsorption capability on Co-containing Y-zelite. *Ion Exchange Adsorp.* **2004**, *20* (3), 254.
(14) Dahlan, I.; Lee, K. T.; Kamaruddin, A. H. Sorption of SO_2 and NO from simulated flue gas over rice husk ash (RHA)/Cao/CeO_2 sorbent: Evaluation of deactivation Kinetic parameters. *J. Hazard. Mater.* **2011**, *185*, 1609.
(15) Liu, Q. Y.; Liu, Z. Y. Carbon supported vanadia for multi-pollutans remvoal from flue gas. *Fuel* **2013**, *108*, 149.
(16) Chatti, R.; Bansiwal, A. K.; Thote, J. A. Amine loaded zeolites for carbon dioxide capture: Amine loading and adsorption studies. *Microporous Mesoporous Mater.* **2009**, *121*, 84.
(17) Gao, X.; Liu, S. Physicochemical properties of metal-doped cativated carbons and relationship with their performance in the removal of SO_2 and NO. *J. Hazard. Mater.* **2011**, *188*, 58.
(18) Shen, C. Z.; Grande, C. A.; Li, P. Adsorption equilibrira and kinetics of CO_2 and N_2 on activated carbon beads. *Chem. Eng. J.* **2010**, *160*, 398.

(19) Chatti, R.; Bansiwal, A. K.; Thote, J. A. Amine loaded zoelites for carbon dioxide capture: Amine loading and adsorption studieds. *Microporous Mesoporous Mater.* **2009**, *121*, 84.
(20) Yang, S. T.; Kim, J.; Ahn, W. S. CO_2 adsorption over ion-exchanged zeolite beta with alkali and alkaline earth metal ions. *Microporous Mesoporous Mater.* **2010**, *135*, 90.
(21) Khelifa, A.; Derriche, Z.; Bengueddach, A. Sorption of carbon dixoide by zeolite X exchanged with Zn^{2+} and Cu. *Microporous Mesoporous Mater.* **1999**, *32*, 199.
(22) Barr, T. L. *Zeolite* **1990**, *10*, 760.
(23) Esquivel, D.; Cruz, A. J.; Sanchidrian, C. J. Local environment and acidity in alkaline and alkaline-earth exchanged β zeolite: Structural analysis and catalytic properties. *Microporous Mesoporous Mater.* **2011**, *142*, 672.
(24) Huang, H. H.; Jiang, X.; Siew, H. L. Oxygen coadsorption and reaction with potassium on MgO thin films grown on Ru (001). *Surf. Sci.* **1998**, *418*, 320.
(25) Huang, H. H.; Jiang, X.; Zou, Z. The oxidation of potassium on MgO (100). *Surf. Sci.* **1998**, *398*, 203.
(26) Tang, Q.; Zhang, Z. G.; Zhu, W. P. SO_2 and NO selective adsorption properties of coal-based activated carbons. *Fuel* **2005**, *84*, 461.
(27) Savara, A.; Sachtler, W. M.; Weitz, E. TPD of NO_2^- and NO_3^- from Na-Y: The relative stabilities of nitrates and nitrites in low temperature $DeNO_x$ catalysis. *Appl. Catal. B: Eviron.* **2009**, *90*, 120.
(28) Torre, C.; Henriques, C.; Ribeiro, F. R. Selective catalytic reuction of NO on copper-exchanged zeolites: the role of the structure of the zeolite in the nature of copper-active sites. *Catal. Today* **1999**, *54*, 407.
(29) Gupta, A.; Gaur, V.; Verma, N. Breakthrough analysis for adsorption of sulfur-dioxide over zeolites. *Chem. Eng. Process* **2004**, *43*, 9.
(30) Srinivasan, A.; Grutzeck, M. W. The adsorption of SO_2 by zeolites synthesized from fly ash. *Environ. Sci. Technol.* **1999**, *33*, 1464.
(31) Xing, N.; Wang, X. P.; Yu, Q. Adsorption performance of zeolites for NO and NO_2. *Chin. J. Catal.* **2007**, *28*, 205.
(32) Klose, W.; Rincon, S. Adsorption and reaction of NO on activated carbon in the presence of oxygen and water vapour. *Fuel* **2007**, *86*, 203.
(33) Frisch, M. J.; Trucks, G. W.; Schlegel, H. B.; et al. *Gaussian 03*, revision C.02; Gaussian, Inc.: Wallingford, CT, 2004.